Available online at www.sciencedirect.com

ScienceDirect

Advances in Space Research 67 (2021) 3807–3818

ADVANCES IN SPACE RESEARCH (a COSPAR publication)

www.elsevier.com/locate/asr

Metrology on-board PROBA-3: The shadow position sensors subsystem

Vladimiro Noce [a,b,*], Davide Loreggia [c], Gerardo Capobianco [c], Silvano Fineschi [c], Alessandro Bemporad [c], Marta Casti [c,d], Steven Buckley [e], Marco Romoli [b], Mauro Focardi [a], Massimiliano Belluso [f], Cédric Thizy [g], Aline Hermans [g], Damien Galano [h], Jorg Versluys [h]

[a] *INAF-Arcetri Astrophysical Observatory, Largo E. Fermi, 5, I-50125 Florence, Italy*
[b] *University of Florence, Department of Physics and Astronomy, Via Sansone 1, I-50019 Sesto Fiorentino, Italy*
[c] *INAF-Turin Astrophysical Observatory, Via Osservatorio, 20, I-10025 Pino Torinese, Italy*
[d] *P/L, Aerospace Technologies and Facilities – ALTEC Torino, Italy*
[e] *ON Semiconductor, 6800 Airport Business Park, Cork, Ireland*
[f] *INAF-Catania Astrophysical Observatory, Via S. Sofia, 78, I-95123 Catania, Italy*
[g] *Centre Spatial de Liege, Av. du Pre Aily, 4031 Liege, Belgium*
[h] *European Space Agency, Keplerlaan 1, 2201 AZ Noordwijk, the Netherlands*

Received 31 January 2020; received in revised form 27 July 2020; accepted 1 August 2020
Available online 18 August 2020

Abstract

PROBA-3 is an ESA mission aimed at the demonstration of formation flying performance of two satellites that will form a giant coronagraph in space. The first spacecraft will host a telescope imaging the solar corona in visible light, while the second, the external occulter, will produce an artificial eclipse. This instrument is named ASPIICS (*Association of Spacecraft for Polarimetric and Imaging Investigation of the Corona of the Sun*). To accomplish the payload's scientific tasks, PROBA-3 will ensure sub-millimeter reciprocal positioning of its two satellites using closed-loop on-board metrology. Several metrology systems will be used and the Shadow Position Sensor (SPS) subsystem senses the penumbra around the instrument aperture and returns the 3-D displacement of the coronagraph satellite, with respect to its nominal position, by running a dedicated algorithm. In this paper, we describe how the SPS works and the choices made to accomplish the mission objectives.

Keywords: Formation-flying; Sun pointing; Coronagraphy; SiPM (Silicon Photomultipliers); SPS (Shadow Position Sensor); On-board metrology

1. Introduction

PROBA (PRoject for On-Board Autonomy) is a series of ESA missions dedicated to in-orbit demonstration of technologies. PROBA-3, in particular (Tarabini-Castellani et al., 2013), is devoted to the validation of formation-flying (FF) techniques (Galano et al., 2019) of two satellites (Figure 1) named, respectively: CSC (Coronagraph S/C, about 340 kg, hosting the Coronagraph Instrument – CI) and OSC (Occulter S/C, 150 kg and shaped as a disk 1.4 m diameter), forming a giant (144 m) Lyot coronagraph (ASPIICS – *Association of Spacecraft for Polarimetric and Imaging Investigation of the Corona of the Sun*) (Renotte et al., 2014) (Renotte et al., 2015) (Galano et al., 2018). The two spacecraft will orbit around Earth on an elliptic path (from 600 km to 60530 km and 59° inclination), allowing periodical observations (6 hours over about 20 of duration of one orbit) of the solar corona (the region immediately above the Sun surface) in optimal conditions. The field of view of the instrument allows to observe the corona from 1.08

* Corresponding author.
E-mail address: vladimiro.noce@inaf.it (V. Noce).

https://doi.org/10.1016/j.asr.2020.08.004
0273-1177/

$R_\odot$ (close to the Sun limb as never done before) up to about 3 $R_\odot$. The launch is scheduled for 2022 from the Kourou space center with a Vega launcher, and the mission will last 2.5 years, including 4 months of commissioning. At its end, the spacecraft will naturally de-orbit into the atmosphere.

The highly elliptic orbit does not permit the continuous remote control from Earth of the spacecraft, then, the GNC (Guidance, Navigation and Control) system will maintain the formation in full autonomy. When passing near Earth, using GPS, PROBA-3 will calculate the relative positioning and velocities of the two spacecraft and will propagate them to next apogee passage, where a suite of metrology systems will gradually permit to reach the observation positioning i.e. the perfect alignment (at sub-millimeter level) of the two spacecraft with respect to the Sun direction. Moreover, the mission will periodically perform the following maneuvers (the OSC moving with respect to the CSC), to validate PROBA-3 formation-flying capabilities:

- resizing (change of ISD - *Intersatellite Distance* down to 25 m and up to 250 m);
- retargeting, consisting in a rigid rotation about the CSC Center-of-Mass up to 30°. Each meter of OSC translation corresponds to a 0.38° rotation of the target line;
- combination of both.

In formation keeping, PROBA-3 will fly in strict formation for about eight hours including formation acquisition and break and allowing scientific observations. Afterwards the two S/C will reach a safe, collision risk-free, reciprocal configuration (about 250 m apart) until approaching the apogee when they will regain the formation at the nominal ISD of 144–146 m (season dependent).

The PROBA-3 mission is designed to execute autonomously its orbital activities without any support from ground for more than seven days (or eight orbits) (see Fig. 2).

The metrology systems involved in precise formation flying are listed in the following table with an indication of the spacecraft on which the different elements are distributed: (see Table 1)

In detail:

- Relative GPS: the S/C positions are calculated on-board, near the perigee, and propagated at the apogee.
- Inter Satellite Link: for long range measurements and data transfer between S/C.
- Visual Based Sensor (VBS): two cameras (wide and narrow-angle) mounted on the OSC dark side and looking at pulsed infrared signals coming from the CSC target.
- Fine Lateral and Longitudinal Sensor (FLLS): a laser beamed from the OSC and reflected by a corner cube on the CSC measures with great accuracy the ISD (300 μm).
- Occulter Position Sensor Emitter (OPSE): three luminous points (LED) placed on the anti-Sun disk of the OSC and imaged on the CI. By observing the position of the OPSE, it is possible to retrieve with very high accuracy the relative pointing direction of the CSC towards the OSC.
- Shadow Position Sensor (SPS, this paper's subject) a crown of eight SiPM sensing the penumbra around the CI aperture.

The two spacecraft are three-axis stabilized by means of thrusters (10 mN cold gas for OSC and 1N monopropellant for CSC) and reaction wheels.

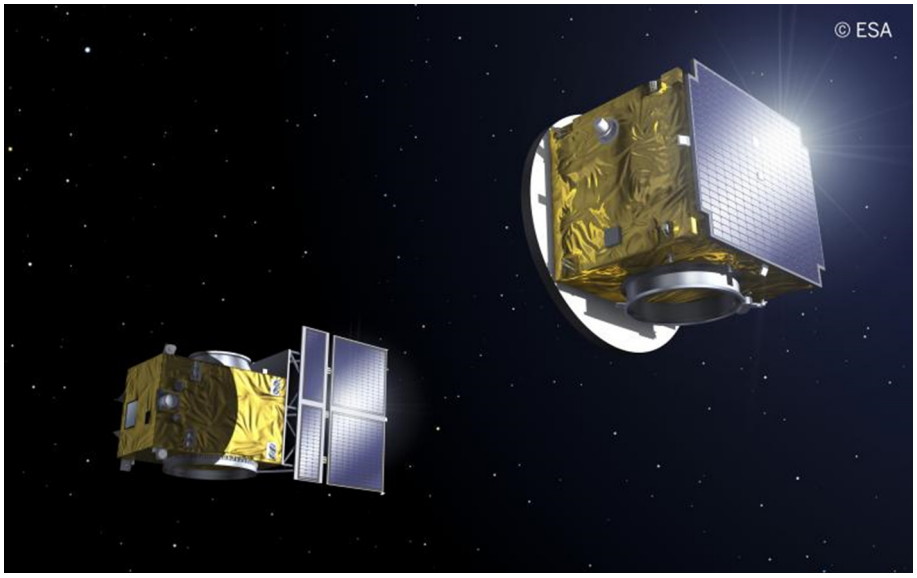

Fig. 1. Picture showing the two S/C composing the PROBA-3 mission, the distance is not in scale (Courtesy ESA).

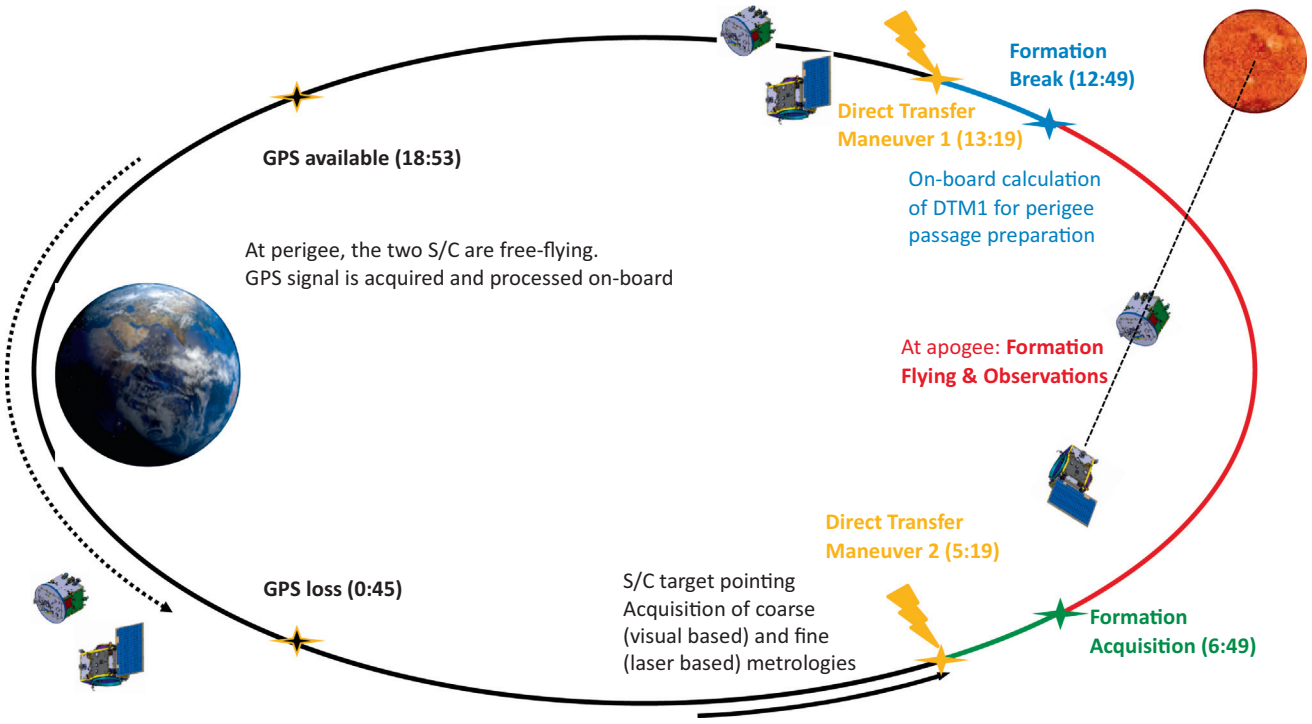

Fig. 2. Description of the different actions that are performed during each operational phase of an orbit (duration 19 h and 38 min) during the PROBA-3 mission.

Table 1
Metrology Sub-systems.

Item	CSC	OSC
Formation Flying units		
OPSE (Occulter Position Sensor Emitter)	Coronagraph detector	3× LED (N + R)
FLLS (Fine Lateral and Longitudinal Sensor)	1× corner cube	Optical Head Unit (Sensors and laser emitters)
SPS (Shadow Position Sensor)	4× SiPM (A + B)	Occulter (D = 1.4 m)
VBS (Visual Based Sensor)	8× IR LED (N + R)	WAC + NAC (N + R)
ISL (Inter Satellite Link)	2× Rx-Tx + 2× antenna	
GNC		
Star trackers	3× OH + 2x electronics	
Gyroscopes	2 × 2	
Sun Sensors	5 (1 Fine and 4 Coarse) redundant cosine sensors	
Rate Sensors	2× Units (3 axis)	
GPS	2× receivers + 2× antennas	
Actuators		
Propulsion Thrusters	2× 8× 1N Monopropellant	2× 12× 10 mN Cold Gas
Reaction Wheels	Pyramid of 4 units	

2. SPS use for calibrating FLLS

The FLLS, although very precise, suffers from attitude errors induced by star trackers (as well as from other sources: thermoelastic deformation of optical bench, corner cube positioning, etc.). The effect of these attitude errors is not observable directly and it is amplified by the large dimensions of the virtual structure (150 m). In-flight calibrations using OPSE and SPS will help to remove many of these errors.

The process of calibration is such:

1. Acquire VBS image (the CSC as seen from OSC) and move OSC until the laser is beamed on the corner cube on CSC
2. Acquire FLLS and move to the approximately correct position (as it is possible to know up to now, here any bias between FLLS and star trackers causes an incorrect measurement)
3. Reduce the ISD in order to place the CSC in shadow, OPSE is acquired letting the aligning of the CSC and the OSC
4. Use OPSE to get into a new, approximately correct position (may require a rotation of OSC).

5. Acquire SPS and, once it is acquired, calibrate FLLS.

Along to the purpose of calibration of the other metrologies, SPS is a metrological system in itself, returning a 3D position of CSC with respect the Sun-to-OSC axis that can be used directly in the FF-GNC loop. It is insensitive to attitude errors, and it is expected to be the most accurate lateral position sensor for coronagraphy. Without SPS, the FF system would not be able to know the position with respect to the umbra with an accuracy better than ~ 5 mm, the minimal value needed for a proper working of ASPIICS even in absence of a longitudinal error. In case a longitudinal error is allowed, this accuracy has to be further increased (see Table 2).

3. SPS readout concept

SPS (Shadow Position Sensor) (Focardi et al., 2016) is the last metrology system to intervene and the most accurate between them (Noce et al., 2017). It is based on the continuous measurement (and a 2 Hz readout cadence) of the penumbra profile around the nominal position and on its fitting with a model of the light expected to be present behind the occulter. The 3-D actual positioning of the center of the entrance pupil of the telescope, placed on the Coronagraph S/C, is calculated with respect to its nominal position i.e. the umbra center at the nominal ISD.

Eight Silicon Photomultipliers (SiPM, 3 × 3 mm, SensL model MicroFB-30035), divided in two independent sets, are placed on a circular PCB, at a constant distance of 55 mm from the center of the coronagraph entrance pupil diaphragm. All signals are amplified and digitized on the PCB itself feeding an on-board algorithm that translates the digital values in absolute 3-D displacements with respect to the nominal position.

When the spacecraft are not in observation mode, the front face of the flange hosting the SPS is covered by a lid (FDA – Front Door Assembly), whose main purpose is to prevent the intrusion of direct Sunlight inside the coronagraph instrument. The FDA has holes pierced on it and, when the door is closed, four sensors are exposed to full Sun and four sensors are protected by neutral density filters transmitting only 1% (ND2) of the light. This set of sensors (A set) will be used to calibrate periodically the sensor responsivity and the electronic chain, by using the full Sun as a "standard candle" (Capobianco et al., 2019) (see Fig. 3).

Before hitting the sensors, the Sun light is filtered in the range 500–660 nm by a band-pass coating deposited on the radiation-hard windows. This interval of wavelengths was

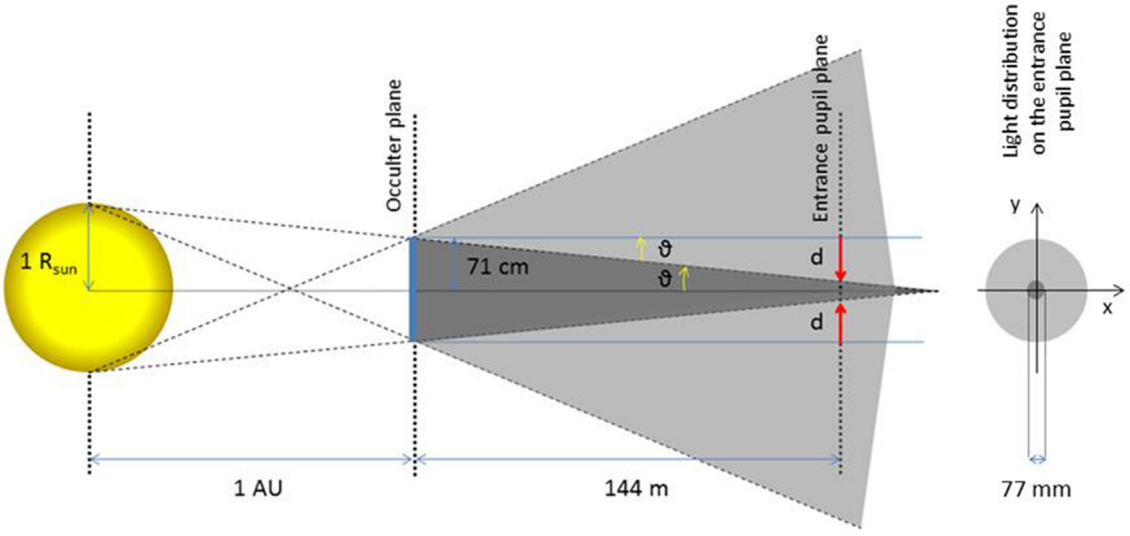

Fig. 3. Image (not in scale) of penumbra (light gray) and umbra (dark gray) in the direction connecting the two spacecraft and on the entrance pupil plane.

Table 2
Proba-3 Pointing and Positioning Requirements.

	Requirement	Value
Absolute Attitude	Pointing	7.1 arc-sec
	Pointing stability (10 s)	2.6 arc-sec
Relative displacement error	@ 40 m	distance 2.2 mm
	@ 150 m	distance 4.9 mm
	@ 250 m	distance 8.1 mm
	Relative velocity error	0.15 mm/s

accurately chosen for a double purpose: first, the sensor's responsivity depends on the temperature and this information is not fed to the algorithm. Reducing the wavelength range, and in particular cutting the longer ones, makes the responsivity pretty much independent from temperature in the whole operation range (28–46 °C). The second reason regards the comparison between the full-Sun (reduced by 1% ND filter) signal and the signal received from a thin crescent of Sun in normal operation. Because of the *limb darkening effect,* the spectral content of the light of the portion of the Sun that we see changes. Cutting the lower part of the spectrum allows us to compare directly the two measurements for calibration purposes.

A two-stage electronics (Noce et al., 2019) converts the photo-current generated by each SiPM in a voltage that is digitized by a 12-bit ADC. The second stage amplifier is used to improve the sensitivity in the lower light range. The difference between opposite sensors measurements is obviously related to the direction and to the amount of displacement from the ideal position. But, in order to translate them in displacement measurements, with the desired performances, these values are fitted to a third-order pseudo-paraboloid with the axis of symmetry parallel to the optical axis. This metrology algorithm (Casti et al., 2019) converts the digital readouts into three spatial coordinates stating how the origin of the reference frame moved from its nominal position.

3.1. Algorithm description:

Several metrology algorithms (Casti et al., 2019) convert the digital readouts into three spatial coordinates that express how the origin of the reference frame M (nominally placed at the center of the coronagrapher's aperture on the CSC, Y and Z on the plane, X pointing to the OSC) moved from its nominal position.

3.2. Linear algorithm (lateral only)

This method is based on a proportionality relation between the difference of the digital reading (R_n) of opposite sensors and the coordinates of the umbra center within the lateral plane. The computation of the Y-Z coordinates is performed using a linear equation, parameterized with reconfigurable coefficients in order to consider any possible occulter distortion.

$$\begin{cases} z_0 = \frac{(R_7 - R_3)}{d_z} \\ y_0 = \frac{(R_1 - R_5)}{d_y} \end{cases} \tag{1}$$

3.3. Pseudo-paraboloid algorithm (lateral)

In order to obtain the performances (50 μm accuracy in a 200 × 20 × 20 mm^3 box), originally requested at the beginning, it was adopted a more refined method based on a third order polynomial equation ("pseudo-para boloid") used to fit the penumbra profile. The coefficients of this curve a, b and c, are reconfigurable and depend on the distance between the two spacecraft (ISD).

$$\begin{cases} z_0 = 2 \cdot \sqrt{-\frac{A}{3}} \cdot cos\left\{ \frac{1}{3} \left[\cos^{-1} \left(\frac{(R_7 - R_3)c^3}{4\sqrt{-\left(\frac{A}{3}\right)^3}} \right) + 4\pi \right] \right\} \\ y_0 = 2 \cdot \sqrt{-\frac{A}{3}} \cdot cos\left\{ \frac{1}{3} \left[\cos^{-1} \left(\frac{(R_1 - R_5)c^3}{4\sqrt{-\left(\frac{A}{3}\right)^3}} \right) + 4\pi \right] \right\} \end{cases} [m] \tag{2}$$

Where:

$$A = c^3 \left(\frac{1}{a} + \frac{2r_{SPS}}{b^2} + \frac{3r_{SPS}^2}{c^3} \right) [m^2] \tag{3}$$

With $r_{SPS} = 55$ mm.

3.4. Longitudinal position computation

The longitudinal coordinate x_0 of the M point is calculated considering a quadratic fitting describing the dependence of the signal present at 55 mm from the coordinate X only. Inverting this relationship:

$$x_0 = \left(\frac{-K - \sqrt{K^2 - 4H(L - R_{55comp})}}{2H} + J \cdot d_0^2 \right) \tag{4}$$

Where:

$$R_{55comp} = R_{0comp} - \Delta R \tag{5}$$

$$d_0^2 = y_0^2 + z_0^2 \tag{6}$$

R_{0comp} (linked to the location x_0 of the occulter center) is the average of four values calculated independently from the radiance values R_n exploiting the knowledge of the y_0 and z_0 coordinates obtained with the previous methods, while H, J, K and L coefficients are reconfigurable.

4. Requirements and SPS design

The required precision in the reconstruction of the positioning of the coronagraph S/C with respect to the center of the umbra cast by the occulter disk at the nominal position is currently stated in two ESA requirements:

4.1. SPS performance requirement

The Shadow Position Sensor (SPS) shall be used to verify that the Coronagraph Instrument's entrance pupil is centered within the umbra cone of the Occulter Disk. At the ISD [...] and within ± 10 mm of the ideal position in lateral and ± 100 mm in range (requirement box), the SPS shall have a lateral measurement accuracy of 500 μm in each axis, and a longitudinal measurement accuracy of 50 mm.

4.2. SPS performance goal

The SPS should be able to return a 3D relative position measurement at reduced performance within a range of ± 50 mm in lateral and ± 500 mm in longitudinal (goal box).

It must be noted, nevertheless, that, at the origin, the performance required was 50 μm for the lateral measurement accuracy and 1 mm for the lateral one. These very stringent needs dictated the design of the electronics as well as the choice of the algorithm.

4.3. Irradiance measurements concept

We based the choice of design parameters on the expected penumbra profile that has been calculated starting from the geometric shape of the portion of Sun seen by each sensor and considering the light diffracted from the occulter edge (Bemporad, 2015) (Baccani et al., 2016). The absolute irradiances and their variations can be translated in requirements on the irradiance range and on the sensitivity of the system:

- The Shadow Position Sensor electronics shall provide meaningful measurements for signals up to the levels of current present in the *goal box* (~38 μA) (Tarabini-Castellani et al., 2013) plus margin.
- The sensitivity needed to detect a longitudinal displacement of 50 mm inside the *requirement box* varies as a function of the position we are considering. The minimum needed sensitivity is 14nA (59nA in nominal position) in an interval of currents comprised between 0.07 and 6.4 μA.
- Note that in the same interval, the needed sensitivity to detect a lateral displacement of 500 μm is larger than the previous one (21 and 110 nA, respectively). If the electronics satisfies the previous point, it will satisfy this, too.

Resuming: the SPS electronics must not saturate up to 38 μA. But, at the same time, for low light levels it must appreciate variations of 14 nA. The following table compares the currents to the digital output, considering that digital numbers are in the interval 0–20475 (4095 × 5) (see Table 3).

4.4. Double stage design description

The final SPS design is based: first, on a transimpedance amplifier capable of covering the entire *goal box* plus a margin and, second, on a non-inverting amplifier, in order to improve the achievable sensitivity and the resolution attainable by the system for lower signals. The current C, generated by the SiPM, is proportional to the irradiance I according an average responsivity of the sensors A (2.60 A/W) and the condition that the light passes through circular pinholes of 2.5 mm diameter. The current C is then transformed in a voltage $V = C \times R_F$ by means of the transimpedance amplifier. At the end, the R_F value can be deduced from the following inequality:

$$(I_{max} + M) \times S \times A \times R_F \leq 5V \tag{7}$$

meaning that the maximum irradiance to be detected (plus a margin) multiplied by the illuminated surface S and the responsivity A must give a current such that, when transamplified by R_F, the output voltage is still in the ADC range. Finally, the feedback resistor has been set to 100 kΩ, allowing the electronics to cover the desired intensity range plus a 30% margin in light levels. The second parameter to be set, namely the non-inverting amplification factor $A_{HG} = 5$, allows to increase the sensitivity of the lower range where more precision is needed (see Fig. 4).

When all the parameters of the electronics have been well defined, we can calculate the expected output counts (DN) in function of the lateral distance from the center of the umbra and at various ISD. The *requirement box* is covered entirely by the high-gain outputs and the sensitivity obtained for lateral and longitudinal displacements (at the nominal ISD), at its lower boundary and around the nominal position are listed in the following table (see Table 4).

The two sets of sensors (A and B) can be switched on and off independently by means of SSR (Solid State Relays) and optocouplers. This ensures the isolation between redundant and nominal power sources, preventing failure propagation, and the accomplishment of the power budget. A 12-bit serial ADC (ADC128S102, working at 4.16 MHz) samples the signals at a rate of 32.5 ksps, then an FPGA operates a running average (256 samples) on the digitized data and provides the proper value, LG or HG, to the algorithm (see Fig. 5).

Table 3
Signal values.

	Distance from center	Current (μA)	Digital readout (DN)
Requirement Box, inner edge	40.9 mm @ISD-100 mm	0.07	30
Nominal position	55 mm @ISD	2.5	1017
Requirement Box, outer edge	69.1 mm @ISD + 100 mm	6.4	2658
Goal box, outer edge	125.5 mm @ISD + 500 mm	~38	~16000

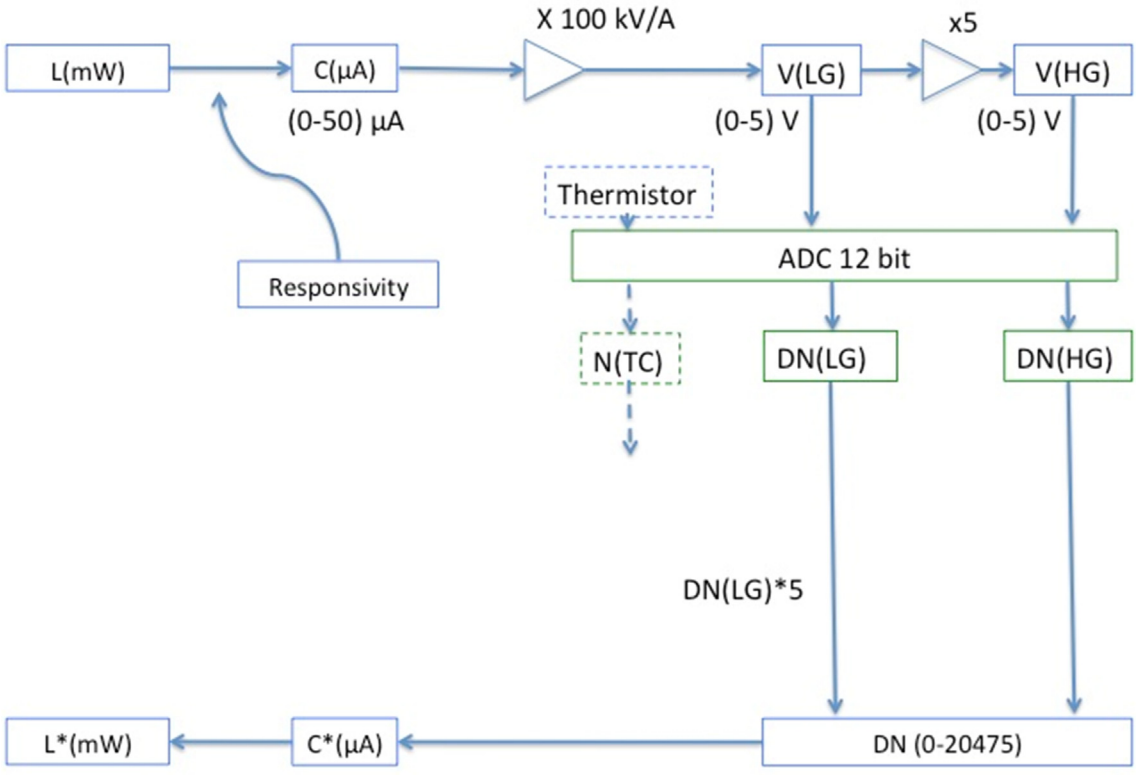

Fig. 4. A visual representation of the logic of measurements taking place in the SPS design.

Table 4
Simulated Sensitivity at Nominal ISD.

	Distance from center	Absolute (DN)	Variation (DN)
Longitudinal, 50 mm	40.9 mm	50	8
	55 mm	1017	23
	69.1 mm	2556	35
Lateral, 500 μm	40.9 mm	50	−8/+17
	55 mm	1017	45
	69.1 mm	2556	50

5. SPS models

Up to now, three demonstration models have been manufactured (Loreggia et al., 2018). Extensive laboratory tests on the first two (a single sensor evaluation board and a complete board equipped with an interface system) allowed us to learn several lessons and to spot potential issues that led to the introduction of important changes:

- Simplification of the design, still keeping the desired performances; introduction of a voltage reference feeding the ADC.
- Insertion of a power switching section isolating the supply voltage sources and switching independently the two sets of sensors for power budget reasons.

5.1. Evaluation board and demonstration model

The original design was based on a three-stage amplification chain. The figure below shows one of the eight sensor chains (see Fig. 6).

The SiPM output photo-current is transformed in a voltage by the transimpedance amplifier TIA. This voltage is amplified once in order to fit the ADC input range and its value is compared to a digital value stored in a look-up table that is used to subtract a programmable voltage pedestal (by means of a DAC – Digital to Analog Converter) to the signal itself.

Two development models were realized using this approach: a single sensor evaluation board (EB) and a complete board equipped with an FPGA-based interface system (DM – Development Model), see figure below (see Fig. 7).

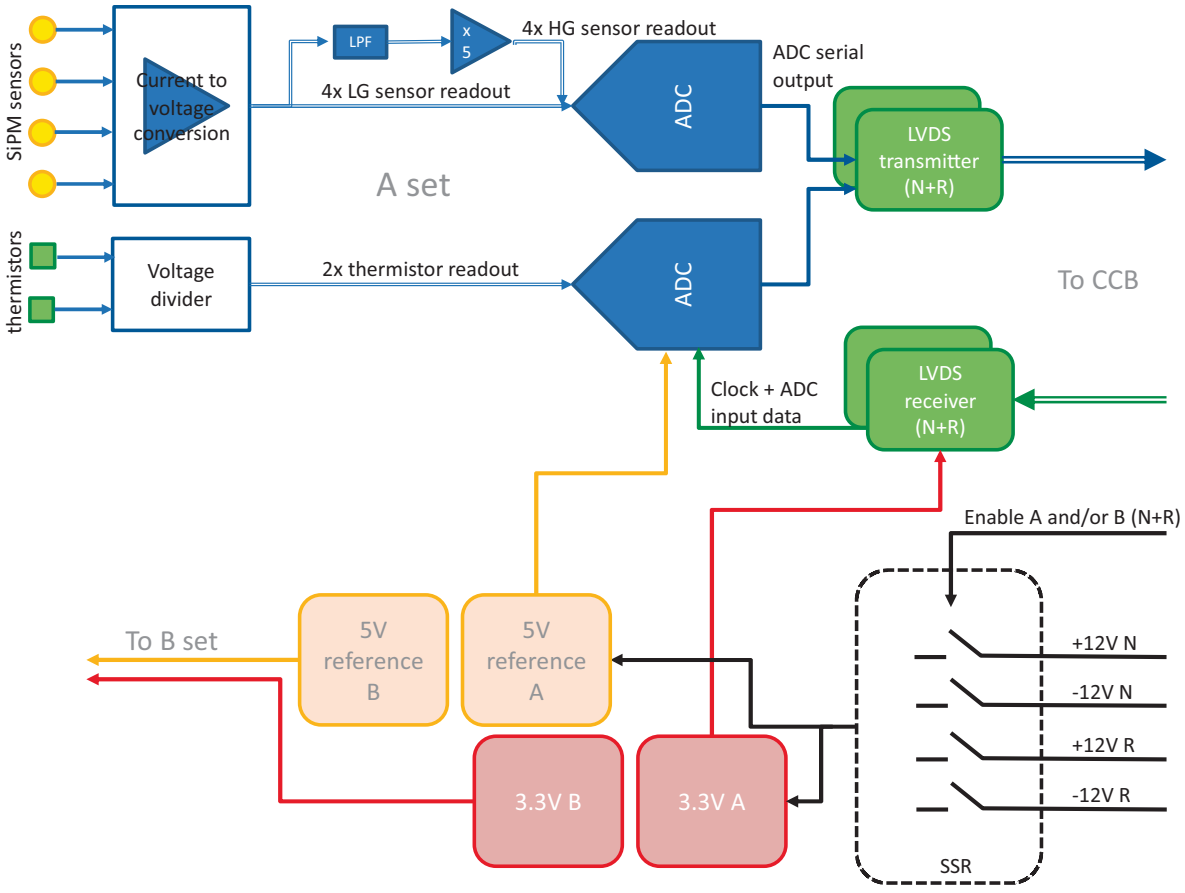

Fig. 5. A scheme of the SPS electronics. Only set A and the section of voltage switching and conversion are shown.

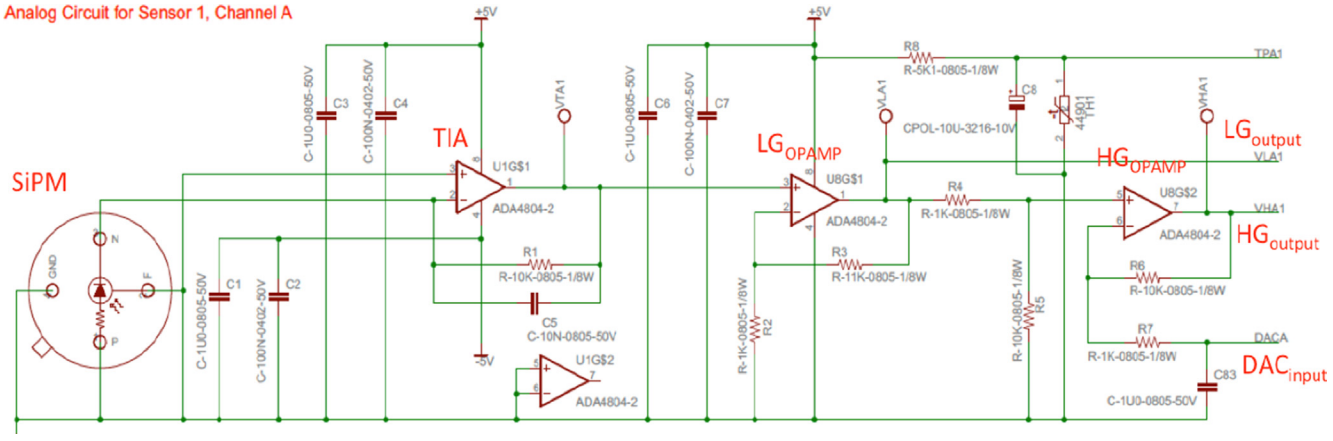

Fig. 6. The amplification chain of one SiPM (previous design).

5.2. Lessons learned from EB and DM measurements and tests

Several electrical and functional tests have been performed on these development models and the outcomes led to significant changes in the electronics, the main ones being:

1. The introduction of a power switching section
2. The adoption of differential transmission lines for sending and receiving data
3. The need of a stable voltage reference on-board for the ADC

An important consequence of the latter point was the direct feeding of ± 12 V to the board and the generation of secondary voltages on-board.

From the point of view of the general design, the most important impact was due to the ESA decision to relax

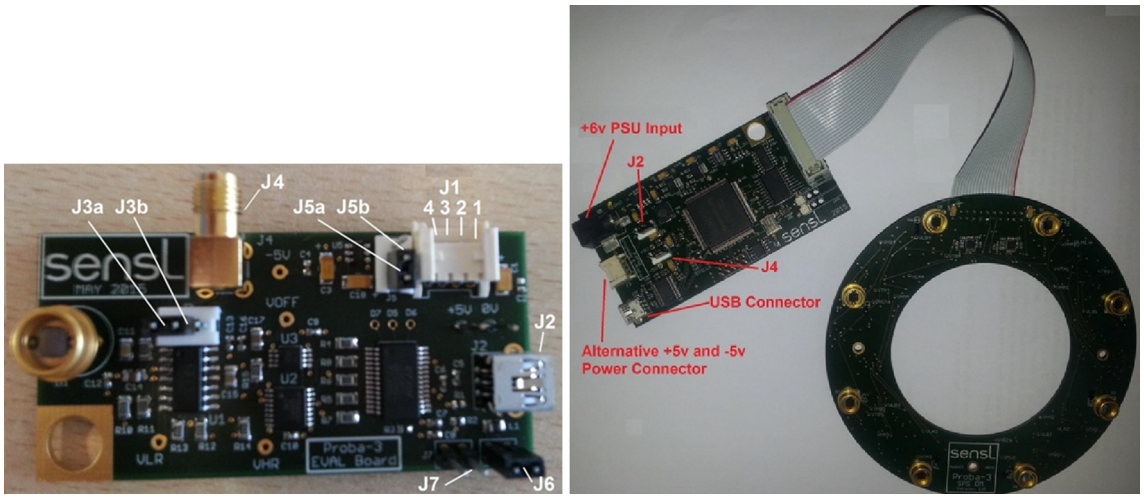

Fig. 7. Left: the single-sensor Evaluation Board. Right: the Development Model with the interface board.

the requirements on lateral (from 50 to 500 μm) and on longitudinal (from 1 to 50 mm) accuracies. This, together with all other considerations, let us to adopt a simplified design that got rid of the DAC and the look-up table round trip complicacies.

5.3. ADM – advanced demonstration model

After the changes in the design at CDR (Critical Design Review) which occurred subsequently thorough investigations on previous development models, INAF decided to produce an intermediate model, not foreseen by the original model philosophy: The Advanced Demonstration Model (ADM) whose three samples were tested in Florence and Catania/Turin labs. This model is adherent to the final design as consolidated in the Critical Design Review, but it is realized with commercial components. It has also the purpose of practicing the test plan, the laboratory setups and the instruments useful also for Engineering Qualification (EQM), and Flight (FM) models' qualification campaigns (see Figs. 8 and 9).

5.4. EQM – Engineering qualification model

The SPS-EQM (Engineering Qualification Model) is the SPS model foreseen by the model philosophy that anticipates the FM construction. It is built on the base of the approved design reported in the CDR data-pack and was subject to functional qualification tests. The qualification followed in part the test plan experienced with the ADM, and its purpose was to verify the proper operation of the EQM readout electronics. The tests were focused on the verification of the electrical compliance, the functional operation and the validation of the absolute performance of the system. A full radiometric characterization will be performed in the future by means of calibrated sources for a complete SPS algorithm qualification (see Figs. 10 and 11)

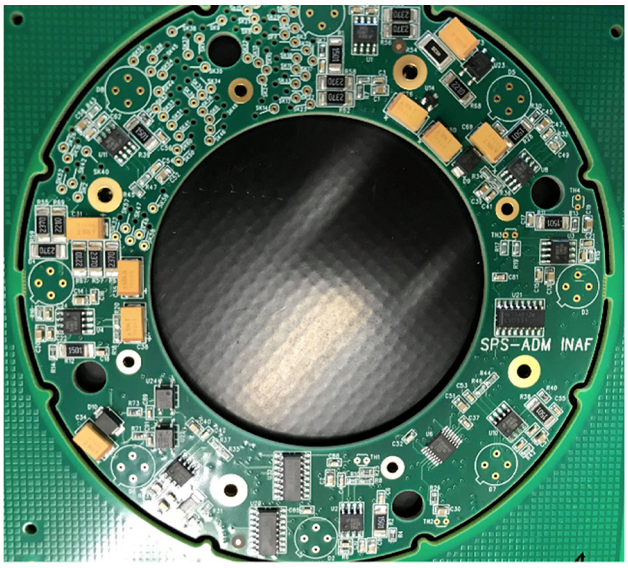

Fig. 8. PROBA-3 Advanced Demonstration Model.

Both ADM and EQM can be interfaced with a FPGA-based board simulating the operations that will be performed by the On-board software. The SPS system and its functions are controlled from a PC by means of a GUI (Graphic User Interface) that reads data and stores them for further analysis.

5.5. EQM tests

EQM was subject to a qualification process that was aimed at verifying the proper operation of the SPS readout electronics. The tests performed were focused on the verification of:

- Electrical and mechanical compliance
- Functional operation
- Environmental testing

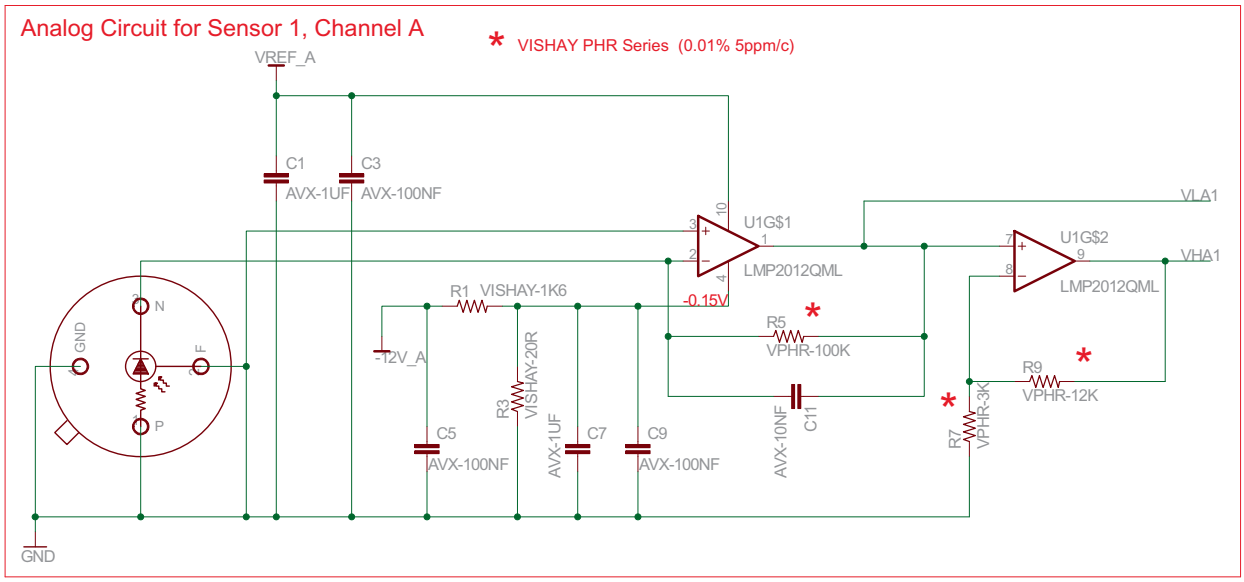

Fig. 9. The amplification chain of one SiPM (current design).

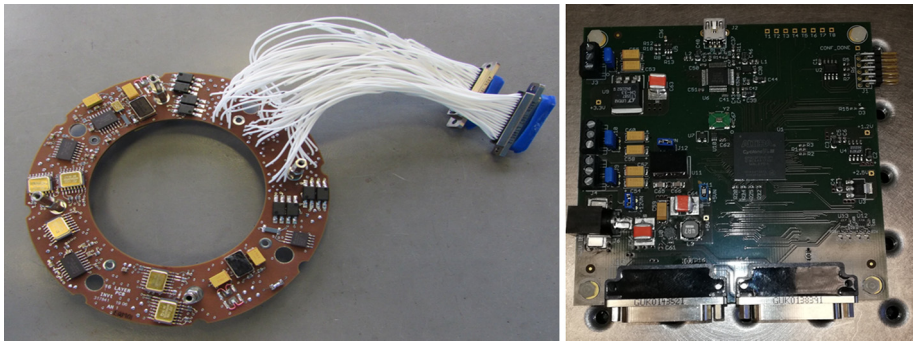

Fig. 10. The EQM with the two 37-pin pigtail connectors and its interface board.

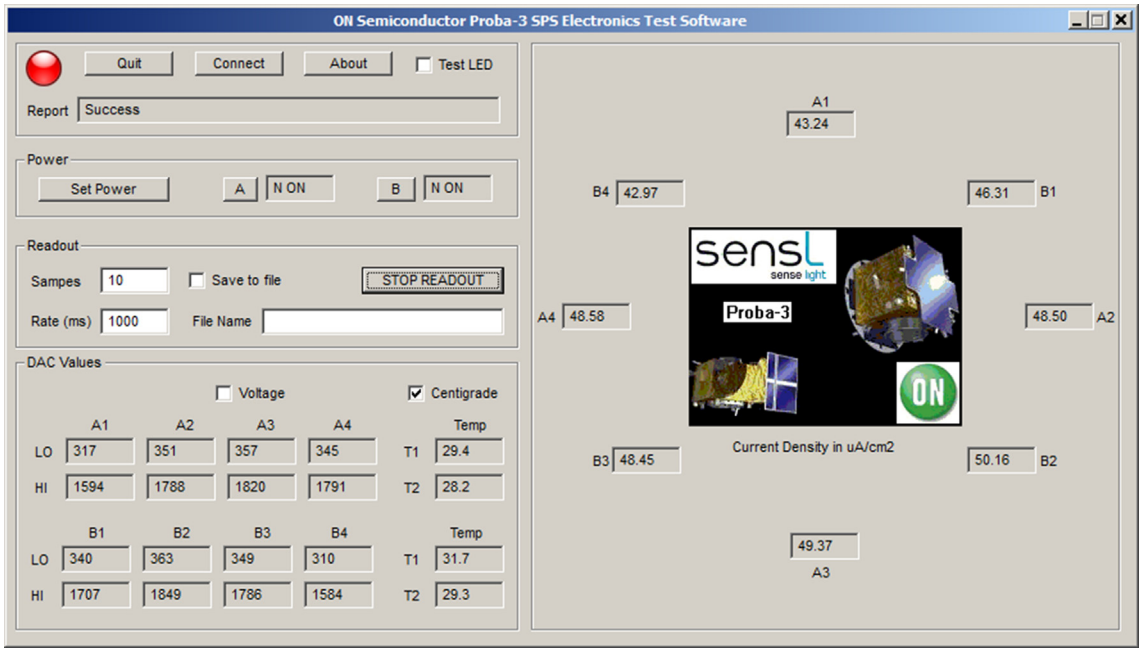

Fig. 11. The ADM/EQM Graphic User Interface.

5.5.1. Mechanical

The PCB inner and outer diameters, the thickness, the mass and the position and diameter of internal holes have been verified. Some minor hardware non-conformances have been highlighted and solved prior FM production. After this, PCB have been subject to electrical, functional and environmental tests.

5.5.2. Electrical

The quality of primary and secondary voltages was measured and the switching capability was tested. Test procedures (Short Functional and Full Functional) have been elaborated for subsequent tests.

5.5.3. Functional

In this phase an absolute calibration was not feasible due to the need of a testbed with radiometric calibrated sources. During qualification tests we used a flat-field light source and a calibrated photodiode in order to, provisionally, at least assess the proportionality of the response and the continuity from high gain to low gain readout (see Fig. 12).

5.5.4. Thermo-vacuum and Vibration

After the electrical and functional tests, the EQM-PCB has been permanently enclosed in the EQM-Flange. On the whole EQM subsystem (SPS + Flange), the thermo-vacuum and vibration qualification have been performed and successfully passed.

The thermal qualification test campaign of the EQM has been done in the IAPS (Rome) thermal vacuum facility, inside an ISO 8 class clean room and consisted of:

- Eight cycles in the qualification temperature range (−30 °C, +89 °C), with a switch on/switch off sequence of the SPS during the first cycle at the non-operative (NOP) temperature limits (−19.6 °C, +78.7 °C);
- Thermal Balance Test, consisting of two cases, hot and cold.

The vibration and pyro-shock tests on the EQM-SPS (PCB + Flange) were completed at SERMS (Terni, Italy) facility. Functional test done before and after vibrations and shocks confirmed the performances of the SPS electronics as verified at the delivery.

In parallel, the SPS system behavior is simulated by a data chain whose purpose is to describe the various steps from spacecraft displacement to illumination levels to electric signals, etc. up to the reconstruction of the position by the algorithm. All these parts are described by models (e.g. MatLab/Simulink modules) and the EQM could replace one or more of these in order to give a realistic response.

6. Error budget

The design performances are summarized in the following table. It should be noted that readout electronics contribution is negligible. The main reason is that the SPS readout system was originally conceived to perform an accuracy 10 × times better (50 × considering the 1 mm longitudinal displacement) and this led to a design performing very well, also considering the strategies adopted to reduce the dependence from temperature.

The main residuals come from the lack of knowledge of the actual shape of the penumbra, that will be the subject

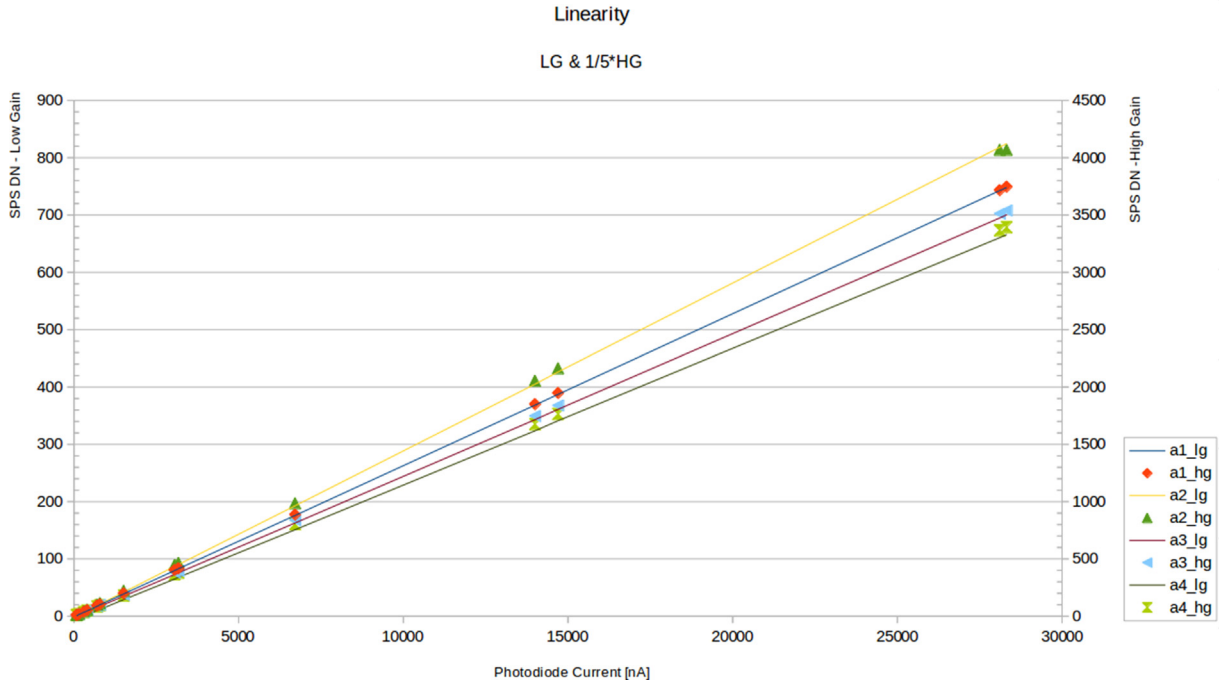

Fig. 12. Plot showing the outputs (LG and HG divided by 5) of four sensors showing the linearity of the response. Little discrepancies can be expected due to quantization, in fact LG values proceed in step of 5.

Table 5
Error budget.

Contribution	Lateral (μm)	Longitudinal (mm)
Metrology System Error Budget		
Readout electronics	1	0.2
Algorithms – Fit of penumbra profile (worst case)	54	20
Ageing + radiation (without periodical calibration)	160	32
In-flight calibration residuals (3-months periodicity)	21	4.2
On-ground calibration residuals	5	1
Uncertainties on the Penumbra Illumination Profile		
Diffraction	600	120
Sunspots	215	8
Total error in absence of Sunspots		
End of Life without penumbra assessment and only initial calibration	>800	176
End of Life with penumbra assessment and periodical calibrations	59	10

of a dedicated in-flight calibration campaign and from the possible presence of spots on the edge of the Sun. The latter contribution could be compensated tuning opportunely the configurable parameters in the algorithm after observations from Earth (see Table 5).

7. Conclusions

In this paper we have described the evolution of the SPS subsystem design on board the PROBA-3 mission prior the Flight Model production. The consolidated design at the CDR milestone was subject to design changes deriving from first models tests and analyses. These preliminary results, compared with the SPS relevant requirements, gave us the opportunity to implement important changes in the electronics and software design in particular in relation to the dependence of this fundamental metrological subsystem from the supplied voltage stability. Furthermore, we described the amplification factors choice criteria deriving from the required sensitivity and dynamic range and how these parameters are connected. An intermediate ADM has been produced in order to practice test activities and procedures useful for the EQM and FM qualification campaign.

Declaration of Competing Interest

The authors declare that they have no known competing financial interests or personal relationships that could have appeared to influence the work reported in this paper.

Acknowledgments

The authors acknowledge the support provided by the PROBA-3 Managerial and Technical Staff of the European Space Agency (ESA) within the contract with CSL (Centre Spatial de Liège) and subcontractors, subscribed for the Payload Instrument design and development (C/D Phases).

References

Baccani, C., Landini, F., Romoli, M., et al., 2016. Preliminary evaluation of the diffraction behind the PROBA 3/ASPIICS optimized occulter. Proc. SPIE Space Telescopes Instrument.: Optical, Infrared, Millimeter Wave 9904 (990450).

Bemporad, A., 2015. Expected penumbra illumination profile and SPS output currents for PROBA-3/ASPIICS. Technical Note, P3-INF-TN-14001.

Capobianco, G., Fineschi, S., Loreggia, D. et al., 2019. The in-flight calibration of the shadow position sensors, optical metrology system of the ESA/PROBA-3 formation flying mission. In: Glasgow, UK, 10th International Workshop on Satellite Constellations and Formation Flying (IWSCFF).

Casti, M., Fineschi, S., Loreggia, D., et al., 2019. Fine positioning algorithm for the ESA PROBA-3 formation flying mission. In: Turin, Italy, IEEE International workshop on Metrology for Aerospace.

Focardi, M., Noce, V., Buckley, S., et al., 2016. The shadow position sensors (SPS) formation flying metrology subsystem for the ESA PROBA-3 mission: present status and future developments. Proc. SPIE 9904 (99044Z).

Galano, D., Buckley, S., Cernica, I., et al., 2018. Development of ASPIICS: a coronagraph based on Proba-3 formation flying mission. In: Proc. SPIE: Space Telescopes and Instrumentation 2018: Optical, Infrared, and Millimeter Wave, 10698 (106982Y).

Galano, D., Jollet, D., Mellab, K., et al., 2019. Proba-3 Precise Formation Flying Mission. In: Glasgow, UK, 10th International Workshop on Satellite Constellations and Formation Flying (IWSCFF).

Loreggia, D., Fineschi, S., Bemporad, A., et al., 2018. Formation flying metrology system for the ESA-PROBA3 mission: the Shadow Positioning Sensors (SPS). Proc. SPIE: Opt. Instrum. Sci., Technol., Appl. 10695 (1069503).

Noce, V., Capobianco, G., Bemporad, A. et al., 2019. Metrology on-board PROBA-3: The Shadow Position Sensors (SPS) subsystem - Design and performance. In: Turin, Italy, IEEE International Workshop on Metrology for Aerospace.

Noce, V., Focardi, M., Buckley, S. et al., 2017. An improved version of the Shadow Position Sensor readout electronics on-board the ESA PROBA-3 mission. In: Proc. of SPIE: Optical Engineering + Applications, 10397 (103971B).

Renotte, E., Alia, A., Bemporad, A., et al., 2015. Design status of ASPIICS, an externally occulted coronagraph for PROBA-3. In: Proc. SPIE: Solar Physics and Space Weather Instrumentation, 9604 (96040A).

Renotte, E., Baston, E.C., Bemporad, A., et al., 2014. ASPIICS: an externally occulted coronagraph for PROBA-3. Design evolution. Proc. SPIE 9143 (91432M).

Tarabini-Castellani, L., Llorente, J.S., Fernández Ibarz, J.M., et al., 2013. Proba-3 mission. Int. J. Space Sci. Eng. 1 (4), 349–366.